frontiers | Frontiers in Molecular Biosciences

TYPE Original Research
PUBLISHED 13 February 2024
DOI 10.3389/fmolb.2024.1350699

OPEN ACCESS

EDITED BY
Laurent Roberto Chiarelli,
University of Pavia, Italy

REVIEWED BY
Sabab Hasan Khan,
The Pennsylvania State University (PSU), United States
Pooja Gopal,
National University of Singapore, Singapore

*CORRESPONDENCE
Dean C. Crick,
dean.crick@colostate.edu

RECEIVED 05 December 2023
ACCEPTED 16 January 2024
PUBLISHED 13 February 2024

CITATION
Fontes FL, Rooker SA, Lynn-Barbe JK, Lyons MA, Crans DC and Crick DC (2024), Pyrazinoic acid, the active form of the anti-tuberculosis drug pyrazinamide, and aromatic carboxylic acid analogs are protonophores.
Front. Mol. Biosci. 11:1350699.
doi: 10.3389/fmolb.2024.1350699

Pyrazinoic acid, the active form of the anti-tuberculosis drug pyrazinamide, and aromatic carboxylic acid analogs are protonophores

Fabio L. Fontes[1,2], Steven A. Rooker[2], Jamie K. Lynn-Barbe[2], Michael A. Lyons[2], Debbie C. Crans[1,3] and Dean C. Crick[1,2]*

[1]Program in Cell and Molecular Biology, Colorado State University, Fort Collins, CO, United States, [2]Mycobacteria Research Laboratories, Department of Microbiology, Immunology and Pathology, Colorado State University, Fort Collins, CO, United States, [3]Department of Chemistry, Colorado State University, Fort Collins, CO, United States

Pyrazinoic acid is the active form of pyrazinamide, a first-line antibiotic used to treat *Mycobacterium tuberculosis* infections. However, the mechanism of action of pyrazinoic acid remains a subject of debate, and alternatives to pyrazinamide in cases of resistance are not available. The work presented here demonstrates that pyrazinoic acid and known protonophores including salicylic acid, benzoic acid, and carbonyl cyanide *m*-chlorophenyl hydrazone all exhibit pH-dependent inhibition of mycobacterial growth activity over a physiologically relevant range of pH values. Other anti-tubercular drugs, including rifampin, isoniazid, bedaquiline, and *p*-aminosalicylic acid, do not exhibit similar pH-dependent growth-inhibitory activities. The growth inhibition curves of pyrazinoic, salicylic, benzoic, and picolinic acids, as well as carbonyl cyanide *m*-chlorophenyl hydrazone, all fit a quantitative structure–activity relationship (QSAR) derived from acid–base equilibria with R^2 values > 0.95. The QSAR model indicates that growth inhibition relies solely on the concentration of the protonated forms of these weak acids (rather than the deprotonated forms). Moreover, pyrazinoic acid, salicylic acid, and carbonyl cyanide *m*-chlorophenyl hydrazone all caused acidification of the mycobacterial cytoplasm at concentrations that inhibit bacterial growth. Thus, it is concluded that pyrazinoic acid acts as an uncoupler of oxidative phosphorylation and that disruption of proton motive force is the primary mechanism of action of pyrazinoic acid rather than the inhibition of a classic enzyme activity.

KEYWORDS

uncoupling, QSAR, growth inhibition, *Mycobacterium tuberculosis*, benzoic acid, salicylic acid, *para*-aminosalicylic acid, picolinic acid

Abbreviations: BDQ, bedaquiline; BEN, benzoic acid; CFZ, clofazimine; CCCP, *N*-(3-chlorophenyl) carbonohydrazonoyl dicyanide; INH, isoniazid; PAS, *p*-aminosalicylic acid; PIC, picolinic acid; POA, pyrazinoic acid; PZA, pyrazinamide; RIF, rifampin; and SAL, salicylic acid. The abbreviation used for the protonated form of each of these compounds is followed by a subscripted N and the deprotonated form a subscripted C; when referring to both forms or when the form present is unclear, a subscript T is used.

10.3389/fmolb.2024.1350699

Introduction

Pyrazinoic acid (POA) is the active form of the prodrug pyrazinamide (PZA), an antibiotic used in combination with other drugs in standard treatment regimens for tuberculosis (TB) infections (World Health Organization, 2018). Multiple reports indicate that the addition of PZA to the various regimens available for TB treatment reduced the average time of treatment from 9–12 months to 6 months (British Thoracic and Tuberculosis Association, 1976; British Thoracic Society, 1984). Therefore, significant effort has been devoted to determining the mechanism of action of POA, a topic that has long been debated (Zhang and Mitchison, 2003; Lamont et al., 2020), and multiple molecular targets have been proposed (Shi et al., 2014; 2011; Kim et al., 2014; Peterson et al., 2015; Njire et al., 2017; Gopal et al., 2020).

Intriguingly, the activity of PZA *in vitro* is pH-dependent (Peterson et al., 2015; Salfinger and Heifets, 1988), and two decades ago, it was suggested that the activity of PZA could be predicted using the Henderson–Hasselbalch equation [HHE, (Zhang and Mitchison, 2003)], a hypothesis which was confirmed recently (Fontes et al., 2020). PZA is deaminated in the bacterial cytoplasm by a nicotinamidase (PncA) forming deprotonated pyrazinoate (POA_C) to exhibit antibacterial activity (Scheme 1) (Konno et al., 1967; Scorpio and Zhang, 1996; Boshoff and Mizrahi, 2000; French et al., 2010). However, of the proposed molecular drug targets, all are cytoplasmic enzymes or activities (Shi et al., 2014; 2011; Kim et al., 2014; Peterson et al., 2015; Njire et al., 2017; Gopal et al., 2020), and none provides an adequate explanation for the pH dependence of PZA activity as *Mycobacterium tuberculosis* maintains cytoplasmic pH homeostasis over an environmental pH range of 5.5–7.3 (Fontes et al., 2020). Recent evidence demonstrated that the growth-inhibitory effect of pyrazinoic acid (POA_N) on *M. tuberculosis* was due to the acid–base equilibrium and indicated that the POA_C formed inside the cell by the activity of PncA must be exposed to the exterior milieu in order to demonstrate a pH effect. However, the chemical nature of a weak acid such as pyrazinoic acid (POA_N) is seldom considered when the mode of action of this drug is investigated. Here, the effects of exposure of *M. tuberculosis* to structural analogs of POA_N and various anti-TB drugs used in the clinic were investigated with the goal of developing a better understanding of the mechanism of action of POA_N.

In solution, the charged, deprotonated POA_C resulting from the deamidation of PZA exists in equilibrium with the neutral, protonated POA_N (Scheme 2; Supplementary Figure S1), and the total pyrazinoic acid (POA_T) concentration in solution consists of the sum of the concentrations of the neutral and charged forms ($POA_N + POA_C$, respectively). The pH-dependent growth inhibitory effect of PZA in *M. tuberculosis in vitro* depends on the differential concentration of POA_N in the bacillary cytoplasm and the environment (Fontes et al., 2020). This observation resulted in the hypothesis that POA_N may act as a protonophore, uncoupling oxidative phosphorylation and leading to a cascade of secondary effects that cause growth arrest and may explain the synergism PZA exhibits with other anti-tubercular drugs.

Chemiosmotic theory postulates that the establishment of a proton electrochemical gradient across the membrane is generated through oxidative processes and then used to generate

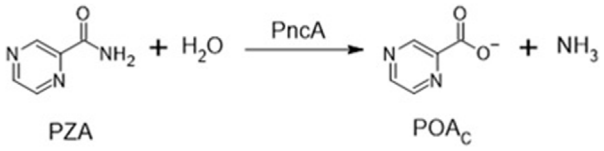

SCHEME 1
Deamidation of pyrazinamide by the endogenous *Mycobacterium tuberculosis* nicotinamide deamidase PncA.

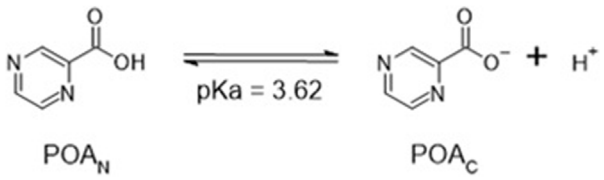

SCHEME 2
Acid–base equilibrium of pyrazinoic acid.

ATP (oxidative phosphorylation) (Mitchell, 1966). Substrate oxidation in the electron transport chain drives the generation of an electrochemical potential, designated as proton motive force (PMF), with two associated components: the electric potential ($\Delta\Psi$), stemming from all charged species on both sides of the membrane, and the proton concentration gradient (ΔpH) across the plasma membrane. The dissipation of one or both of these components can lead to the disruption of PMF, although compensatory mechanisms have been reported (Bakker and Mangerich, 1981; Booth, 1985).

Uncouplers of oxidative phosphorylation are compounds able to, through various mechanisms, decouple substrate oxidation from the phosphorylation of ADP to form ATP (Hanstein, 1976). Protonophores are compounds that can dissipate both $\Delta\Psi$ and ΔpH by shuttling protons across the membrane uncoupling oxidative phosphorylation. Carbonyl cyanide *m*-chlorophenyl hydrazone (Figure 1) is a well-characterized example of such a compound. In solution, the neutral, protonated *N*-(3-chlorophenyl) carbonohydrazonoyl dicyanide ($CCCP_N$) exists in equilibrium with its charged, deprotonated form, 1-(3-chlorophenyl)-2-(dicyanomethylene) hydrazine-1-ide ($CCCP_C$), and the total carbonyl cyanide *m*-chlorophenyl hydrazone ($CCCP_T$) is the sum of the concentrations of each species. The equilibrium between $CCCP_N$ and $CCCP_C$ drives the activity as a protonophore, in an acidic environment outside the cell, a fraction of $CCCP_T$ exists as $CCCP_N$. The membrane permeability to $CCCP_N$ is greater than that of $CCCP_C$ (LeBlanc, 1971), which results in $CCCP_N$ being more likely to cross the membrane than $CCCP_C$. Upon exposure to the cytoplasmic environment, the higher pH alters the acid–base equilibrium between $CCCP_N$ and $CCCP_C$ as described by the HHE, releasing protons in the cytoplasm. Therefore, $CCCP_N$ disrupts ΔpH if the flux into the cells is greater than the flux of protons generated by the cell in the opposite direction (Mitchell, 1966). Furthermore, since the flux of $CCCP_C$ occurs without the use of a counterion, the uncoupling event caused by $CCCP_T$ is electrogenic, leading to the dissipation of $\Delta\Psi$.

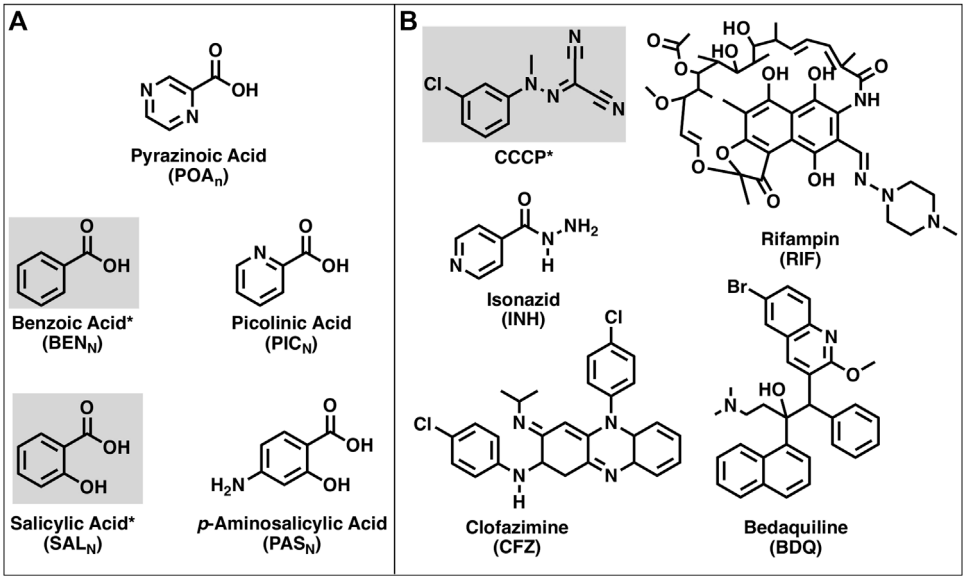

FIGURE 1
Structures of the compounds used in this work. **(A)** Structures of pyrazinoic acid and analogs. **(B)** Structures of CCCP and various anti-TB drugs. Compounds highlighted and indicated by an asterisk are known protonophores.

The activity of protonophores, in general, is pH-dependent as the membrane penetration of the protonated form of the compound is dependent on concentration, which, in turn, depends on the total protonophore concentration and the pH of the solution as described by the HHE. Protonophores have simple structural requirements for activity that include a protonatable (weak acid) group for activity and a hydrophobic moiety, often aromatic, that increases membrane solubility (Hanstein, 1976; Heytler, 1979). Many small, hydrophobic weak acids have been shown to be protonophores (Dilger and McLaughlin, 1979; McLaughlin and Dilger, 1980; Gutknecht, 1990; Norman et al., 2004; Peters et al., 2016). These include compounds structurally similar to POA such as benzoic acid and salicylic acid (Figure 1). Other weak acids that are structurally similar to POA include picolinic acid and the anti-TB drug *p*-aminosalicylic acid (Lehmann, 1946a; 1946b). The availability of these compounds and anti-mycobacterial drugs (isoniazid, clofazimine, bedaquiline, and rifampin) that have known mechanisms of action, as well as protonatable groups (Figure 1) that could, in theory, provide protonophoric activity, has enabled the present studies into the potential mechanism of action of PZA.

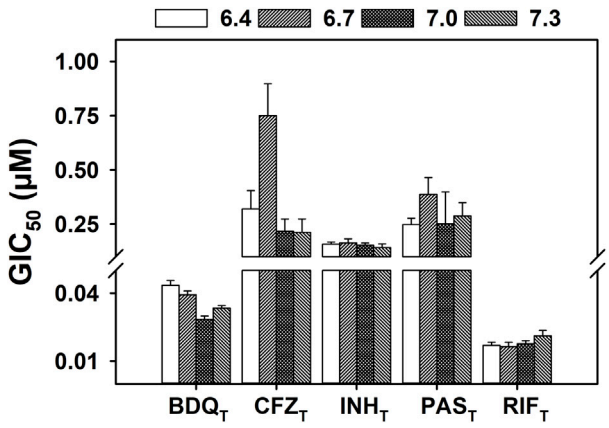

FIGURE 2
Effect of pH on the growth inhibition of *M. tuberculosis* by known anti-tubercular drugs. *M. tuberculosis* H37Ra were incubated at 37°C in supplemented 7H9 broth with a range of concentrations of the specified antibiotic. The OD_{600} was measured every 24 h for 5 days, with growth rates calculated by determining the slope at each time point. The GIC_{50} (concentration of compound that inhibits 50% of the growth rate) values were calculated with the growth rates of day 5, from four independent biological replicates. The GIC_{50} values extracted from the E_{max} model regression are presented at each external pH tested (6.4–7.3). The error bars of each bar correspond to the standard deviation calculated during the regression. Linear regression analysis of the data can be found in Supplementary Material.

Results

Mycobacterium tuberculosis H37Ra pH-dependent growth inhibition

The pH-dependent activity of POA_T *in vitro* has been established in multiple reports (Salfinger and Heifets, 1988; Zhang et al., 2002; Peterson et al., 2015; Fontes et al., 2020). However, the effect of pH on the activity of other anti-tubercular drugs is rarely considered, despite the pathogenesis models for *M. tuberculosis* suggesting exposure to a range of pH environments in the host (Effros and Chinard, 1969; Nielson et al., 1981; Nyberg K et al., 1992; Masuda et al., 2015; Irwin et al., 2016; Lanoix et al., 2016).

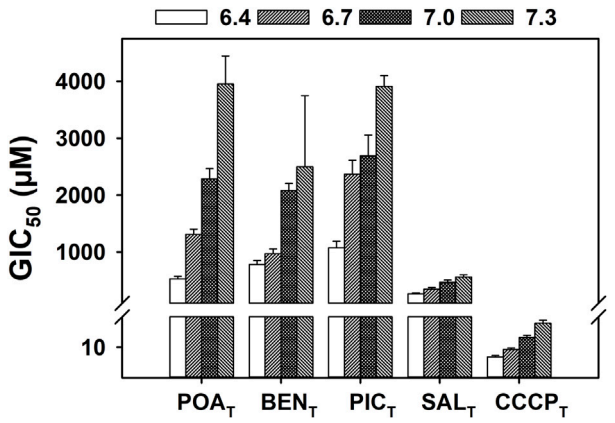

FIGURE 3
Effect of pH on the growth inhibition of *M. tuberculosis* by POA_T, structural analogs of POA_T, and $CCCP_T$. Mycobacterial cultures were grown in supplemented 7H9 broth at 37°C and incubated with a range of concentration of the specified compound for 5 days. The OD_{600} was measured every 24 h, and growth rates were determined by calculating the slope of the growth curve at each time point. The GIC_{50} (concentration of compound that inhibits 50% of the growth rate) values shown were determined with the growth rates of day 5 regression of an E_{max} model for each environmental pH value (6.4–7.3), using four biological replicates. The error bars shown correspond to the standard deviation extracted during the regression. Linear regression analysis of the data can be found in Supplementary Material.

Figure 2 shows the concentrations of the anti-TB drugs *para*-aminosalicylic acid (PAS_T), bedaquiline (BDQ_T), clofazimine (CFZ_T), isoniazid (INH_T), and rifampin (RIF_T) responsible for 50% inhibition of *M. tuberculosis* H37Ra growth (GIC_{50}) over a small range of environmental pH values (6.4–7.3) corresponding to those likely to be encountered in a host organism. All of the anti-mycobacterial drugs shown in Figure 2 have different molecular targets, and, with the exception of BDQ_T (Hards et al., 2018), there is no evidence reported in the literature of ionophoric activity by any of the drugs. Linear regression analysis (Supplementary Table S1) of the data shown in Figure 2 demonstrates that the compounds tested exhibit little or no pH-dependent activity against *M. tuberculosis*, over the pH range tested.

Figure 3 shows the GIC_{50} values of POA_T and analogs other than PAS_T (Figure 2), as well as $CCCP_T$ over the pH range of 6.4 and 7.3. POA_T, SAL_T, BEN_T, PIC_T, and $CCCP_T$ all exhibit a linear pH-dependent increase in GIC_{50} as the pH increases with R^2 values of > 0.9 (Supplementary Table S1). Additionally, $CCCP_T$ exhibits the highest efficacy in growth inhibition of all the compounds shown in Figure 3, with SAL_T showing the lowest pH-dependent GIC_{50} values among the POA_T analogs (including POA_T). All the compounds shown in Figure 3 also exhibited higher GIC_{50} values than the results for the compounds shown in Figure 2, including the POA_T analog PAS_T.

Modeling pH-dependent activity in *Mycobacterium tuberculosis* H37Ra

Quantitative structure–activity relationship (QSAR) models have previously been used to determine the activity of drugs or poisons with pH-dependent properties. The model presented in Eq. 1 (*Materials and methods*) was adapted from the work of Könemann and Musch (1981) and derived from acid–base equilibrium chemistry (Supplementary Equations S1–14; Supplementary Figure S1, S2). The GIC_{50} values obtained during the drug susceptibility assays were fit to the model (Eq. 1), and the coefficients T_N and T_C were extracted. T_N is the inverse of the concentration of the protonated (neutral) form of the compound tested responsible for 50% of the growth inhibition, and T_C is the inverse of the concentration of the deprotonated form of the compound tested responsible for 50% of the growth inhibition caused by the anionic species. Thus, both T_N and T_C are expressed as μM^{-1}. The coefficients T_N and T_C and the coefficient of determination (R^2) of the fit to the model for each of the compounds used are presented in Table 1. As expected, the compounds that showed no pH-dependent activity did not fit the QSAR model; however, the compounds with clear pH-dependent activities fit the model with R^2 values greater than 0.9. The modeled behavior of $CCCP_T$-, POA_T-, SAL_T-, BEN_T-, and PIC_T-treated bacterial growth is similar, suggesting similar pH-dependent responses. Figure 4 shows graphic representations of the fits, including the experimentally measured GIC_{50} points, of $CCCP_T$, PAS_T, POA_T, and SAL_T, as a function of the environmental pH used for each GIC_{50} determination. Moreover, all of the compounds with high R^2 scores have values of T_N that are much greater than T_C (Table 1), indicating a higher efficacy of the protonated form of the compounds and/or a mechanistic requirement for the formation of the protonated form (the latter being reported to be true for the protonophoric activity of both $CCCP_T$ and SAL_T) (Kasianowicz et al., 1984; Norman et al., 2004).

Cytoplasmic acidification by structural analogs of pyrazinoic acid in *Mycobacterium tuberculosis* H37Ra

Previous work described POA_T-induced acidification of the cytoplasm of *M. tuberculosis* H37Ra and suggested the uncoupling of proton motive force by POA_N (Fontes et al., 2020). Similarly, PZA has been shown to acidify the mycobacterial cytoplasm (Peterson et al., 2015; Santucci et al., 2022). However, it was not clear that cytoplasmic acidification was a specific effect of POA_T or of anti-TB drugs and protonophores in general. Figure 5 shows the change in the pH gradient between the cytoplasm and the exterior environment (ΔpH) across a range of environmental pH values when the mycobacteria cultures were exposed to $CCCP_T$, PAS_T, POA_T, or SAL_T. $CCCP_T$, POA_T, and SAL_T cause cytoplasmic acidification in a concentration-dependent manner over the range of effective growth inhibition of each compound. In each case, higher efficiency of acidification was observed at the lowest environmental pH tested. However, PAS_T, which does not show pH-dependent growth inhibition activity, does not acidify the cytoplasm.

Discussion

pH-dependent drug susceptibility in *Mycobacterium tuberculosis* H37Ra

The effect of environmental pH on the activity of non-PZA anti-mycobacterial drugs is seldom studied. The drugs used in this work were chosen as they inhibit a range of molecular targets in *M.*

TABLE 1 QSAR model coefficients.

Compound	pK_a[a]	T_N (μM^{-1})	T_C (μM^{-1})	R^2
No pH-dependent activity				
BDQ_T	8.91	24 ± 2	360 ± 160	0.30
CFZ_T	6.63	0 ± 2	6 ± 1	0.30
INH_T	3.35	0 ± 840	6.3 ± 0.4	0.01
PAS_T	3.68	100 ± 460	4.0 ± 0.5	0.01
RIF_T	6.55	50 ± 7	60 ± 4	0.00
pH-dependent activity				
POA_T	3.62	1.10 ± 0.09	0 ± 0.0001	0.96
BEN_T	4.08	0.20 ± 0.02	0.0003 ± 0.0001	0.94
PIC_T	5.52	0.007 ± 0.001	0.0001 ± 0.0001	0.91
SAL_T	2.79	10 ± 0.5	0.0015 ± 0.0001	0.98
$CCCP_T$	5.81	0.60 ± 0.02	0.050 ± 0.003	0.98

[a]pK_a values were obtained through Chemicalize (www.chemicalize.com). For compounds with multiple pK_a values, the pK_a closest to neutral pH was used for calculations.

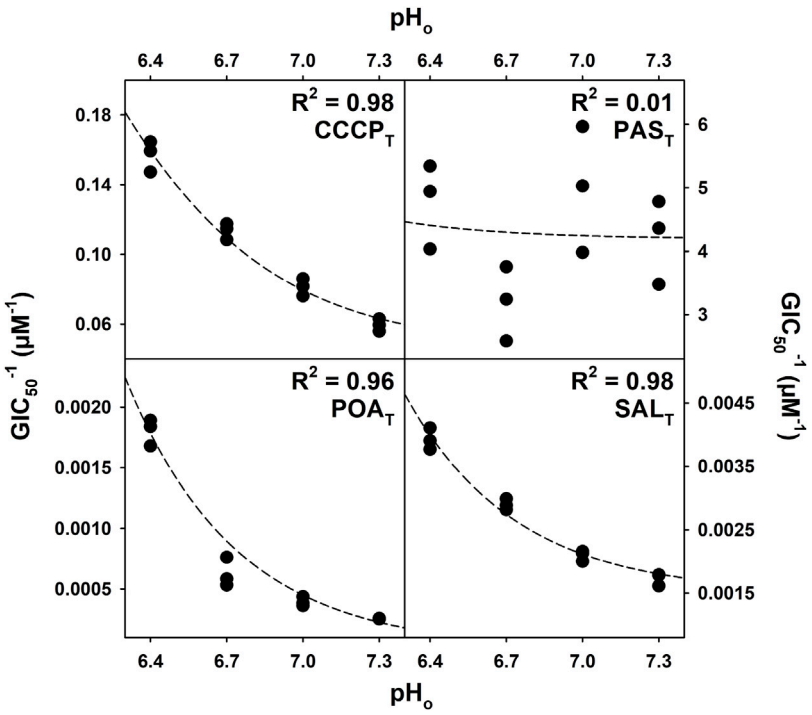

FIGURE 4
Regression of the QSAR model for $CCCP_T$, PAS_T, POA_T, and SAL_T. The GIC_{50} (concentration of compound that inhibits 50% of the growth rate) values (averages of three biological replicates) obtained during the drug susceptibility assay were fit to the model described by Eq. 1. The R^2 values were calculated based on the residuals of the regression, and the curves generated with the coefficients were determined during the regression.

tuberculosis. Both BDQ_T and CFZ_T target energy production, albeit with different modes of action (Yano et al., 2010; Hards et al., 2015), while INH_T has been linked to multiple targets, including cell wall biosynthesis inhibition, nucleic acid synthesis inhibition, and reactive oxygen and nitrogen species generation (Gangadharam et al., 1963; Winder et al., 1970; Takayama et al., 1972; Shoeb et al., 1985; Wengenack and Rusnak, 2001; Sipe et al., 2004; Timmins et al., 2004). PAS_T is reported to inhibit the folate pathway after endogenous conversion into the active form (Chakraborty et al., 2013; Zheng et al., 2013), and RIF_T is a well-described, broad-spectrum inhibitor of DNA-dependent RNA polymerase (Lancini et al., 1969). As shown in Figure 2, none of

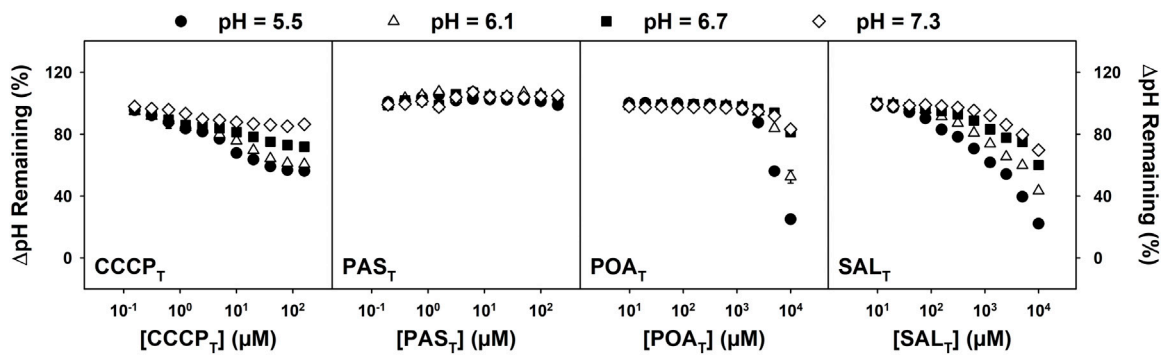

FIGURE 5
Effects of $CCCP_T$, PAS_T, POA_T, and SAL_T on ΔpH over a range of external pH values. *M. tuberculosis* H37Ra cells were incubated in MMA buffer containing 0.5 μM BCECF-AM at the indicated pH and concentration of the desired analog for 30 min. Fluorescence was measured at 37°C with excitation at 440 and 485 nm and emission recorded at 540 nm The percentage of ΔpH remaining was estimated with the BCECF's 485/440 ratio after 30 min of incubation with analog divided by the estimated ΔpH (using pH 7.4 as the cytoplasmic pH); the untreated (DMSO control) was considered 100%. Values shown are the averages of four biological replicates +/− standard deviation for each concentration of compound (in most cases, the error bars are buried within the symbols used).

the anti-mycobacterial drugs mentioned above exhibit pH-dependent increase in the activity as the pH was lowered within the range of environmental pH values tested. The observations of Bartek et al. (2016) support the results shown here for RIF_T, but for the remaining antibiotics mentioned above, no previous reports on their activity at different environmental pH values were available.

The weak acids, POA_T and $CCCP_T$, and the structural analogs of POA_T, other than PAS_T, all exhibited pH-dependent growth inhibition (Figure 3), in contrast to the results shown for the anti-TB drugs in Figure 2. That is, POA_T, BEN_T, SAL_T, PIC_T, and $CCCP_T$ all demonstrate similar patterns of increasing GIC_{50} as the culture pH is increased over a range of 6.4–7.3. The results imply that these five weak acids likely act via a similar mechanism. Of these compounds, BEN_T, SAL_T, and the structurally unrelated $CCCP_T$ are well-known and -characterized protonophores (Levitan and Barker, 1972; Neumcke and Bamberg, 1975; McLaughlin and Dilger, 1980; Kasianowicz et al., 1984; Gutknecht, 1990; Norman et al., 2004; Naven et al., 2013; Peters et al., 2016), suggesting that POA_N also acts as a protonophore, as previously hypothesized (Fontes et al., 2020).

Modeling pH-dependent activity in *Mycobacterium tuberculosis* H37Ra

The QSAR model represented by Eq. 1 was first used as a model for the pH-dependent toxicity of phenols in fish (Tabata, 1962; Könemann and Musch, 1981). Phenols, such as 2,4-dinitrophenol, are also known protonophores and uncouple oxidative phosphorylation (Mitchell, 1966; Naven et al., 2013; Childress et al., 2018; Kotova and Antonenko, 2022). The theoretical framework of the model accounts for the independent toxicity of the protonated and deprotonated forms of uncouplers, expressed by the coefficients T_N and T_C, respectively.

Equation 1 was used to determine how well the growth inhibition data for *M. tuberculosis* H37Ra suspensions exposed to anti-tubercular drugs, known protonophores, and weak acids fit the model of protonophoric activity at pH values of 6.4, 6.7, 7.0, and 7.3. The coefficients extracted, when the GIC_{50} values obtained at different environmental pH values for each of the compounds used were fit to the model, are shown in Table 1. The growth inhibition data for the compounds exhibiting pH-dependent activity (Figure 3) fit the model well with R^2 values greater than 0.9 in all cases. However, the data for those compounds showing no dependence on the pH of the culture medium (Figure 2) do not fit the model. The results of the non-linear regression analysis of growth inhibition data for $CCCP_T$, PAS_T, POA_T, and SAL_T fit to the model, as represented graphically in Figure 4.

The coefficients presented in Table 1 are consistent with the observation that POA_N is the active form of PZA (Fontes et al., 2020) as the coefficient T_N is orders of magnitude greater than T_C. The negligible value of T_C (relative to T_N) indicates that the contribution of the deprotonated POA_C to growth inhibition is also negligible, and the observable effect relies solely on the concentration of the protonated form (POA_N). Similarly, the structurally unrelated $CCCP_T$ and POA_T analogs, other than PAS_T, follow the same pattern, further supporting the hypothesis of a common mechanism of action.

The concentration of POA_N responsible for 50% of the growth inhibition ($1/T_N$) corresponds to ~0.9 μM, a value consistent with the concentration of POA_N responsible for 50% of mycobacterial growth inhibition reported previously (Fontes et al., 2020). The corresponding concentrations for SAL_N, BEN_N, PIC_N, and $CCCP_N$ are 0.1, 5.0, 140, and 1.7 μM, respectively. Thus, POA_N is twice as effective at inhibiting *M. tuberculosis* growth as $CCCP_N$. Moreover, the inverse T_N concentration for SAL_N is ~0.1 μM, which would make SAL_N the best compound at inhibiting mycobacterial growth via a protonophoric mechanism. However, the low pK_a values of POA_T and SAL_T, 3.62 and 2.79, respectively, dictate that to achieve the concentrations of POA_N and SAL_N required to inhibit 50% of growth in environments near pH neutrality, the concentrations of POA_T and SAL_T must be orders of magnitude higher. In addition, given the higher pK_a of $CCCP_T$ (5.81), concentrations of total

compound are closer to the $CCCP_N$ concentration needed to achieve a similar effect. As a result, the concentration of $CCCP_T$ required to inhibit 50% of bacterial growth is orders of magnitude lower than the concentrations of POA_T and SAL_T. However, it is essential to remember that the activity of a protonophore is not solely dependent on pKa. If one plots $1/T_N$ vs. pKa for the pH-dependent compounds used in this work and conducts a linear regression analysis, the resulting R^2 value is less than 0.3. This is likely due, at least in part, to the observation that the rate of PMF dissipation is dependent on the rate of diffusion of the anionic form of the protonophore across the membrane rather than the rate of diffusion of the neutral form in the other direction, which is much greater (McLaughlin and Dilger, 1980). Nonetheless, the results strongly suggest that POA_N acts as a protonophore, given all the similarities described with the known protonophores $CCCP_N$, BEN_N, and SAL_N and the fact that it is unlikely that these compounds would all bind to the same molecular target with similar affinity (resulting GIC_{50} values in the 0.1–5 μM range).

Figure 4 also shows the poor fit obtained for PAS_T growth inhibition data, which reflects the lack of pH dependence presented in Figure 2. PAS_T is a weak acid analog of POA_T, as are SAL_T, BEN_T and PIC_T, which might be expected to have a similar pH behavior and mechanism of action. Nevertheless, the drug susceptibility assays and the QSAR model used here indicate otherwise. This is in agreement with the report that PAS_T inhibits the folate pathway in *M. tuberculosis* after conversion to hydroxyl-dihydropteroate with an MIC_{50} of 0.4 μM. (Zheng et al., 2013). The existence of an endogenous cytosolic molecular target causes bacterial growth inhibition of *M. tuberculosis* at concentrations orders of magnitude lower than those where a protonophoric activity would be observable given the PAS_T pKa of 3.25. Thus, the QSAR model is sensitive to the presence of high-affinity, cytosolic molecular targets.

Similarly, the drug susceptibility assays and the QSAR model used here did not indicate that BDQ_T had pH-dependent or ionophoric activity, observations which are supported by Haagsma et al. (2011), even though BDQ_T was reported to act as an H^+/K^+ antiporter ionophore in *E. coli* membrane vesicles (Hards et al., 2018). In *M. tuberculosis*, BDQ_T inhibits the F_1F_0-ATP synthase, binding to the a-c subunit of the F_0 complex of the ATP synthase and leading to depletion of ATP (Hards et al., 2015). However, *E. coli* ATP synthase lacks the BDQ_T-binding site (Preiss et al., 2015), and the concentrations needed to disrupt PMF in *E. coli* were 30–300-fold higher than the BDQ_T MIC in *M. tuberculosis*. (Hards et al., 2018).

Cytoplasmic acidification by structural analogs of pyrazinoic acid in *Mycobacterium tuberculosis* H37Ra

Consistent with a lack of pH dependence and the QSAR analysis, PAS_T causes no change in the mycobacterial transmembrane ΔpH over the range of concentrations that generates PAS_T-induced growth inhibition. However, Figure 5 shows that cytosolic acidification is apparent when *M. tuberculosis* H37Ra cultures are treated with POA_T, SAL_T, and $CCCP_T$. This is consistent with the previous observations that POA_T causes rapid cytosolic acidification and dissipation of ΔΨ in *M. tuberculosis*. The cytosolic acidification caused by $CCCP_T$ is supported by observations described in the work of Peterson et al. (2015) and Fontes et al. (2020). Zhang et al. (2003) showed similar GIC_{50} values for BEN_T and SAL_T to the values presented here, but they observed no change in the internal pH caused by the two compounds (Zhang et al., 2003). However, these researchers did demonstrate that BEN_T and SAL_T induced ΔΨ disruption in *M. tuberculosis* H37Ra.

The curves presented in Figure 5 suggest that the mechanism of acidification of the cytoplasm by $CCCP_T$ is potentially distinct from that of POA_T and SAL_T. This may be a reflection of the different protonophoric mechanisms reported for $CCCP_T$ and SAL_T (Neumcke and Bamberg, 1975; McLaughlin and Dilger, 1980; Kasianowicz et al., 1984; Gutknecht, 1990; Norman et al., 2004). The mechanism of $CCCP_T$ action (termed A^-) involves the permeation of the protonated $CCCP_N$ through the membrane, the release of the proton upon arrival in the cytoplasm, and subsequent diffusion of the deprotonated $CCCP_C$ through the membrane to the extracellular medium, where $CCCP_C$ can be protonated regenerating $CCCP_N$, and the cycle may begin again (Neumcke and Bamberg, 1975; McLaughlin and Dilger, 1980; Kasianowicz et al., 1984). The uncoupling mechanism of SAL_T has been shown to be distinct from the A^- mechanism (McLaughlin and Dilger, 1980; Gutknecht, 1990; Norman et al., 2004). The SAL_T mechanism, termed AHA^- (or HA_2^-), involves the protonated form of the uncoupler permeating the membrane and releasing a proton on the cytoplasmic side of the membrane, just as described with the A^- mechanism. However, the AHA^- mechanism requires the deprotonated form to establish a heterodimer with a protonated form of itself, forming an anionic dimer (in the case of SAL_T, it requires the SAL_C to form a complex with a molecule of SAL_N) (Neumcke and Bamberg, 1975; McLaughlin and Dilger, 1980). The dimer is, then, able to permeate the membrane, and the deprotonated form of the uncoupler can reach the extracellular medium, where it is available to be protonated again and to initiate a new cycle. Both mechanisms acidify the cytoplasm and are electrogenic, altering both ΔΨ and ΔpH and disrupting PMF (Kasianowicz et al., 1984; Gutknecht, 1992; Norman et al., 2004). In both mechanisms, the concentration of each weak acid must be such that the effective proton conductance is greater than the sum of all other membrane conductance; in addition, the buffers used, solubility in and diffusion through the unstirred water layers adjacent to the membrane, the electrostatic potentials at the membrane–solution interface, the thickness of the bilayer, and the dielectric constant of the membrane all modify the protonophore activity of each weak acid (McLaughlin and Dilger, 1980). While SAL_T has many other reported mechanisms of action (Klessig et al., 2016), the evidence presented here indicates that SAL_T behaves solely as a protonophore in *M. tuberculosis*, and the data suggest that the protonophoric activity of POA_T may have a similar AHA^- mechanism.

Previous reports have shown the susceptibility of *M. tuberculosis* H37Ra and *M. smegmatis* to growth inhibition by SAL_T and BEN_T, among other weak acids (Zhang et al., 2003). Furthermore, the activity of SAL_T and BEN_T was shown to exhibit sterilizing activity against *M. tuberculosis* H37Ra (Wade and Zhang, 2006). However, the literature on the impact of SAL_T or aspirin, the prodrug form of SAL_T used therapeutically, in TB infections is scarce and somewhat controversial (Byrne et al., 2007a; Byrne et al., 2007b; Eisen et al., 2013; Vilaplana et al., 2013). While PZA exhibits activity *in vivo*, the integration of the antibiotic in the standard regimen for TB

infections only occurred after the discovery of the synergism between PZA and RIF_T (British Thoracic and Tuberculosis Association, 1976; British Thoracic Society, 1984). Aspirin and SAL_T, however, were shown to antagonize the activity of multiple anti-tubercular drugs (Schaller et al., 2002). Still, these studies were conducted in neutral pH environments, where SAL_T is less effective, and therefore, the nature of the drug–drug interactions between SAL_T and other antibiotics deserves further investigation. Studies conducted on mice seem to agree on the mild antagonism between SAL_T and INH_T, although an increase in bacterial load clearance with a combination of aspirin and INH_T was also observed (Byrne et al., 2007a). Moreover, SAL_T was shown to synergize with PZA in a murine model (Byrne et al., 2007b), and evidence of improved outcome in patients undergoing treatment with PZA (plus INH_T and ethambutol) when aspirin was added to the regimen exists (Horsfall et al., 1979; Schoeman et al., 2011).

In conclusion, the data presented suggest that pyrazinoic acid acts as an uncoupler of oxidative phosphorylation and that the disruption of proton motive force is the primary mechanism of action of pyrazinoic acid rather than the inhibition of a classic enzyme activity.

Materials and methods

The reagents used in this work were purchased from Sigma-Aldrich, except when noted. Middlebrook 7H9 broth was purchased from Becton Dickinson and albumin from GoldBio. The fluorescent dye used in the cytosolic acidification assay was obtained from Invitrogen. All reagents were used without further purification and were, at least, of reagent grade.

Mycobacterium tuberculosis H37Ra culture methods

M. tuberculosis H37Ra cultures were grown as reported elsewhere (Fontes et al., 2020). In brief, frozen glycerol stocks of *M. tuberculosis* H37Ra were thawed and used to inoculate the Middlebrook 7H9 medium, which was supplemented with oleic acid-albumin-dextrose (OAD, 10% v/v), 0.1% v/v tyloxapol, and 0.2% w/v casamino acids (supplemented 7H9 broth). The pH of the medium was adjusted with hydrogen chloride or sodium hydroxide, when needed, and verified in all cases. The culture flasks were incubated at 37°C, under constant agitation. The cells were harvested when an optical density of 600 nm (OD_{600}) between 0.6 and 0.8 was observed. Further processing of the cultures was carried out according to the requirements of individual assays.

pH-dependent growth inhibition of *Mycobacterium tuberculosis* H37Ra

The growth inhibition activity of anti-tubercular drugs and POA_T analogs was determined, as described previously (Gruppo et al., 2006). Cells of *M. tuberculosis* H37Ra were grown and harvested, with subsequent centrifugation using a Beckman CS-6R centrifuge at 1,500 × g, and then washed with fresh culture medium (supplemented 7H9 broth). The pH of the culture medium was adjusted as described above to obtain pH values ranging from 6.4 to 7.3 in 0.3 unit intervals. Cells were resuspended in the culture medium at the desired pH and incubated until an OD_{600} between 0.6 and 0.8 was reached, as a way to acclimatize the bacilli to the pH of the medium, as described elsewhere (Fontes et al., 2020). The cells were then harvested, centrifuged as above, and washed with fresh medium at the desired pH value. Aliquots of 198 µL of resuspended cells at an OD_{600} of 0.1 were transferred to 96-well microtiter plates containing one zirconia bead per well (diameter approximately 1 mm) to assist with agitation and aeration. Aliquots of 2 µL of a range of concentrations of drug dissolved in dimethyl sulfoxide (DMSO) or water (for BEN_T), including an aliquot containing no drug as a blank, were added to the plate, and the OD_{600} was recorded using a BioRad Benchmark Plus plate reader. The OD_{600} was determined over 5 days, with readings every 24 h. Incubation between time points occurred at 37°C with constant rocking of the plates within a sealed plastic bag containing a damp paper towel to maintain humidity and prevent evaporation. Growth rates were determined by the calculation of the slope of the growth curve at each time point. The calculation of the concentration required to inhibit 50% of growth was carried out using a non-linear four-parameter E_{max} regression model.

Modeling uncoupling activity in *Mycobacterium tuberculosis*

Multiple QSAR models have been proposed to determine the activity of analogs of poisons or drugs. However, the impact of pH in the activity of these compounds is seldom taken into consideration. Based on the work of Tabata (1962), Könemann and Musch (1981) derived a model that accounts for the specific activity of each form of an ionizable compound, which is shown in Eq. 1. The derivation of the model is provided in Supplementary Material.

$$\frac{1}{GIC_{50}} = T_N \cdot \frac{10^{-pH}}{10^{-pH} + 10^{-pK_a}} + T_C \cdot \frac{10^{-pK_a}}{10^{-pH} + 10^{-pK_a}}, \quad (1)$$

where GIC_{50} corresponds to the concentration (total, independent of the protonation state) of a compound required to inhibit 50% of growth, T_N corresponds to the inverse of the concentration of the protonated form of the compound required to cause 50% inhibition of the effect, and T_C is the inverse of the concentration of the deprotonated form of the compound required to cause 50% inhibition. The pH term corresponds to the environmental pH at which the GIC_{50} value was obtained, and pK_a corresponds to the pK_a of the protonated form of the compound.

The GIC_{50} values obtained in the drug susceptibility assay described above were fit to the model described by Eq. 1 with an algorithm created in R. As T_N and T_C correspond to concentrations and, therefore, have biochemical meaning, the algorithm was designed to restrain the values of the coefficients to only values equal or above zero. The coefficients obtained from the fit are reported in Table 1 with standard errors obtained from the fit.

The coefficient of determination was calculated with the residuals of the fit.

Effect of pyrazinoic acid on the internal pH of *Mycobacterium tuberculosis* H37Ra cells

The assessment of the internal pH of mycobacterial cells by analogs of POA_T was performed, as reported previously (Fontes et al., 2020). *M. tuberculosis* H37Ra cultures were grown as described above, and the cells were harvested by centrifugation and washed twice with MMA buffer (a mixed buffer consisting of 25 mM MES, 25 mM MOPS, and 50 mM AMP, prepared as previously communicated) (Fontes et al., 2020). Cells were resuspended in MMA buffer at the desired pH to an OD_{600} of 0.3, and aliquots of 196 µL were transferred into a black-walled 96-well titer plate with one zirconia bead in each well. Background fluorescence was recorded at 37°C for 10 min (in 2 min intervals) on a BioTek Synergy HT (excitation at 440 nm and 485 nm and emission at 540 nm), followed by the addition of 0.5 µM of 2′,7′-bis-(2-carboxyethyl)-5-(and-6)-carboxyfluorescein acetoxymethyl ester (BCECF-AM) to the cells. Fluorescence was recorded for 30 min. Aliquots of 2 µL of a range of concentrations of the desired analog of POA_T dissolved in DMSO (with DMSO without drug serving as a blank) were then added to the cultures, and fluorescence was recorded for another 30 min.

Data availability statement

The raw data supporting the conclusion of this article will be made available by the authors, without undue reservation.

Author contributions

FF: conceptualization, data curation, formal analysis, investigation, methodology, validation, visualization, writing–original draft, and writing–review and editing. SR: investigation and writing–review and editing. JL-B: writing–review and editing. ML: conceptualization, data curation, visualization, and writing–review and editing. DCs: supervision and writing–review and editing. DCk: conceptualization, formal analysis, funding acquisition, methodology, project administration, resources, visualization, writing–original draft, and writing–review and editing.

Funding

The authors declare that financial support was received for the research, authorship, and/or publication of this article. This work was funded by NIH/NIAID grants AI119567 and AI049151.

Conflict of interest

The authors declare that the research was conducted in the absence of any commercial or financial relationships that could be construed as a potential conflict of interest.

Publisher's note

Supplementary material

The Supplementary Material for this article can be found online at: https://www.frontiersin.org/articles/10.3389/fmolb.2024.1350699/full#supplementary-material

References

Bakker, E. P., and Mangerich, W. E. (1981). Interconversion of components of the bacterial proton motive force by electrogenic potassium transport. *J. Bacteriol.* 147, 820–826. doi:10.1128/JB.147.3.820-826.1981

Bartek, I. L., Reichlen, M. J., Honaker, R. W., Leistikow, R. L., Clambey, E. T., Scobey, M. S., et al. (2016). Antibiotic bactericidal activity is countered by maintaining pH homeostasis in *Mycobacterium smegmatis*. *mSphere* 1, 001766–e216. doi:10.1128/mSphere.00176-16

Booth, I. R. (1985). Regulation of cytoplasmic pH in bacteria. *Microbiol. Mol. Biol. Rev.* 49, 359–378. doi:10.1128/mr.49.4.359-378.1985

Boshoff, H. I. M., and Mizrahi, V. (2000). Expression of *Mycobacterium smegmatis* pyrazinamidase in *Mycobacterium tuberculosis* confers hypersensitivity to pyrazinamide and related amides. *J. Bacteriol.* 182, 5479–5485. doi:10.1128/JB.182.19.5479-5485.2000

British Thoracic and Tuberculosis Association (1976). Short-course chemotherapy in pulmonary tuberculosis: a controlled trial by the British Thoracic and Tuberculosis Association. *Lancet* 2, 1102–1104. doi:10.1016/S0140-6736(76)91085-0

British Thoracic Society (1984). A controlled trial of 6 months' chemotherapy in pulmonary tuberculosis Final report: results during the 36 months after the end of chemotherapy and beyond. *Br. J. Dis. Chest* 78, 330–336. doi:10.1016/0007-0971(84)90165-7

Byrne, S. T., Denkin, S. M., and Zhang, Y. (2007a). Aspirin antagonism in isoniazid treatment of tuberculosis in mice. *Antimicrob. Agents Chemother.* 51, 794–795. doi:10.1128/AAC.01145-06

Byrne, S. T., Denkin, S. M., and Zhang, Y. (2007b). Aspirin and ibuprofen enhance pyrazinamide treatment of murine tuberculosis. *J. Antimicrob. Chemother.* 59, 313–316. doi:10.1093/jac/dkl486

Chakraborty, S., Gruber, T., Barry, C. E., Boshoff, H. I., and Rhee, K. Y. (2013). Para-aminosalicylic acid acts as an alternative substrate of folate metabolism in *Mycobacterium tuberculosis*. *Science* 339, 88–91. doi:10.1126/science.1228980

Childress, E. S., Alexopoulos, S. J., Hoehn, K. L., and Santos, W. L. (2018). Small molecule mitochondrial uncouplers and their therapeutic potential. *J. Med. Chem.* 61, 4641–4655. doi:10.1021/acs.jmedchem.7b01182

Dilger, J., and McLaughlin, S. (1979). Proton transport through membranes induced by weak acids: a study of two substituted benzimidazoles. *J. Membr. Biol.* 46, 359–384. doi:10.1007/BF01868755

Effros, R. M., and Chinard, F. P. (1969). The *in vivo* pH of the extravascular space of the lung. *J. Clin. Invest.* 48, 1983–1996. doi:10.1172/JCI106164

Eisen, D. P., McBryde, E. S., and Walduck, A. (2013). Low-dose aspirin and ibuprofen's sterilizing effects on *Mycobacterium tuberculosis* suggest safe new

adjuvant therapies for tuberculosis. *J. Infect. Dis.* 208, 1925–1927. doi:10.1093/infdis/jit476

Fontes, F. L., Peters, B. J., Crans, D. C., and Crick, D. C. (2020). The acid–base equilibrium of pyrazinoic acid drives the ph dependence of pyrazinamide-induced *Mycobacterium tuberculosis* growth inhibition. *ACS Infect. Dis.* 6, 3004–3014. doi:10.1021/acsinfecdis.0c00507

French, J. B., Cen, Y., Vrablik, T. L., Xu, P., Allen, E., Hanna-Rose, W., et al. (2010). Characterization of nicotinamidases: steady state kinetic parameters, classwide inhibition by nicotinaldehydes, and catalytic mechanism. *Biochemistry* 49, 10421–10439. doi:10.1021/bi1012518

Gangadharam, P. R. J., Harold, F. M., and Schaefer, W. B. (1963). Selective inhibition of nucleic acid synthesis in *Mycobacterium tuberculosis* by isoniazid. *Nature* 198, 712–714. doi:10.1038/198712b0

Gopal, P., Sarathy, J. P., Yee, M., Ragunathan, P., Shin, J., Bhushan, S., et al. (2020). Pyrazinamide triggers degradation of its target aspartate decarboxylase. *Nat. Commun.* 11, 1661. doi:10.1038/s41467-020-15516-1

Gruppo, V., Johnson, C. M., Marietta, K. S., Scherman, H., Zink, E. E., Crick, D. C., et al. (2006). Rapid microbiologic and pharmacologic evaluation of experimental compounds against *Mycobacterium tuberculosis*. *Antimicrob. Agents Chemother.* 50, 1245–1250. doi:10.1128/AAC.50.4.1245-1250.2006

Gutknecht, J. (1990). Salicylates and proton transport through lipid bilayer membranes: a model for salicylate-induced uncoupling and swelling in mitochondria. *J. Membr. Biol.* 115, 253–260. doi:10.1007/BF01868640

Gutknecht, J. (1992). Aspirin, acetaminophen and proton transport through phospholipid bilayers and mitochondrial membranes. *Mol. Cell. Biochem.* 114, 3–8. doi:10.1007/BF00240290

Haagsma, A. C., Podasca, I., Koul, A., Andries, K., Guillemont, J., Lill, H., et al. (2011). Probing the interaction of the diarylquinoline TMC207 with its target mycobacterial ATP synthase. *PLOS ONE* 6, e23575. doi:10.1371/journal.pone.0023575

Hanstein, W. G. (1976). Uncoupling of oxidative phosphorylation. *Biochim. Biophys. Acta BBA - Rev. Bioenerg.* 456, 129–148. doi:10.1016/0304-4173(76)90010-0

Hards, K., McMillan, D. G. G., Schurig-Briccio, L. A., Gennis, R. B., Lill, H., Bald, D., et al. (2018). Ionophoric effects of the antitubercular drug bedaquiline. *Proc. Natl. Acad. Sci.* 115, 7326–7331. doi:10.1073/pnas.1803723115

Hards, K., Robson, J. R., Berney, M., Shaw, L., Bald, D., Koul, A., et al. (2015). Bactericidal mode of action of bedaquiline. *J. Antimicrob. Chemother.* 70, 2028–2037. doi:10.1093/jac/dkv054

Heytler, P. G. (1979). "[58] Uncouplers of oxidative phosphorylation," in *Methods in enzymology, biomembranes Part F: bioenergetics: oxidative phosphorylation* (Cambridge: Academic Press), 462–472. doi:10.1016/0076-6879(79)55060-5

Horsfall, P. A. L., Plummer, J., Allan, W. G. L., Girling, D. J., Nunn, A. J., and Fox, W. (1979). Double blind controlled comparison of aspirin, allopurinol and placebo in the management of arthralgia during pyrazinamide administration. *Tubercle* 60, 13–24. doi:10.1016/0041-3879(79)90051-5

Irwin, S. M., Prideaux, B., Lyon, E. R., Zimmerman, M. D., Brooks, E. J., Schrupp, C. A., et al. (2016). Bedaquiline and pyrazinamide treatment responses are affected by pulmonary lesion heterogeneity in *Mycobacterium tuberculosis* infected C3HeB/FeJ mice. *ACS Infect. Dis.* 2, 251–267. doi:10.1021/acsinfecdis.5b00127

Kasianowicz, J., Benz, R., and McLaughlin, S. (1984). The kinetic mechanism by which CCCP (carbonyl cyanide m-chlorophenylhydrazone) transports protons across membranes. *J. Membr. Biol.* 82, 179–190. doi:10.1007/BF01868942

Kim, H., Shibayama, K., Rimbara, E., and Mori, S. (2014). Biochemical characterization of quinolinic acid phosphoribosyltransferase from *Mycobacterium tuberculosis* H37Rv and inhibition of its activity by pyrazinamide. *PLOS ONE* 9, e100062. doi:10.1371/journal.pone.0100062

Klessig, D. F., Tian, M., and Choi, H. W. (2016). Multiple targets of salicylic acid and its derivatives in plants and animals. *Front. Immunol.* 7, 206. doi:10.3389/fimmu.2016.00206

Könemann, H., and Musch, A. (1981). Quantitative structure-activity relationships in fish toxicity studies (Part 2): the influence of pH on the QSAR of chlorophenols. *Toxicology* 19, 223–228. doi:10.1016/0300-483X(81)90131-1

Konno, K., Feldmann, F. M., and McDermott, W. (1967). Pyrazinamide susceptibility and amidase activity of tubercle bacilli. *Am. Rev. Respir. Dis.* 95, 461–469. doi:10.1164/arrd.1967.95.3.461

Kotova, E. A., and Antonenko, Y. N. (2022). Fifty years of research on protonophores: mitochondrial uncoupling as a basis for therapeutic action. *Acta Naturae* 14, 4–13. doi:10.32607/actanaturae.11610

Lamont, E. A., Dillon, N. A., and Baughn, A. D. (2020). The bewildering antitubercular action of pyrazinamide. *Microbiol. Mol. Biol. Rev.* 84, e00070-19. doi:10.1128/mmbr.00070-19

Lancini, G., Pallanza, R., and Silvestri, L. G. (1969). Relationships between bactericidal effect and inhibition of ribonucleic acid nucleotidyl-transferase by rifampicin in *Escherichia coli* K-12. *J. Bacteriol.* 97, 761–768. doi:10.1128/JB.97.2.761-768.1969

Lanoix, J.-P., Ioerger, T., Ormond, A., Kaya, F., Sacchettini, J., Dartois, V., et al. (2016). Selective inactivity of pyrazinamide against tuberculosis in C3HeB/FeJ mice is best explained by neutral pH of caseum. *Antimicrob. Agents Chemother.* 60, 735–743. doi:10.1128/AAC.01370-15

LeBlanc, O. H. (1971). The effect of uncouplers of oxidative phosphorylation on lipid bilayer membranes: carbonylcyanidem-chlorophenylhydrazone. *J. Membr. Biol.* 4, 227–251. doi:10.1007/BF02431973

Lehmann, J. (1946a). Determination of pathogenicity of tubercle bacilli by their intermediate metabolism. *Lancet* 1, 14–15. doi:10.1016/S0140-6736(46)91184-1

Lehmann, J. (1946b). *para*-aminosalicylic acid in the treatment of tuberculosis. *Lancet* 12, 15–16. doi:10.1016/S0140-6736(46)91185-3

Levitan, H., and Barker, J. L. (1972). Salicylate: a structure-activity study of its effects on membrane permeability. *Science* 176, 1423–1425. doi:10.1126/science.176.4042.1423

Masuda, M., Sato, T., Sakamaki, K., Kudo, M., Kaneko, T., and Ishigatsubo, Y. (2015). The effectiveness of sputum pH analysis in the prediction of response to therapy in patients with pulmonary tuberculosis. *PeerJ* 3, e1448. doi:10.7717/peerj.1448

McLaughlin, S. G., and Dilger, J. P. (1980). Transport of protons across membranes by weak acids. *Physiol. Rev.* 60, 825–863. doi:10.1152/physrev.1980.60.3.825

Mitchell, P. (1966). Chemiosmotic coupling in oxidative and photosynthetic phosphorylation. *Biol. Rev.* 41, 445–502. doi:10.1111/j.1469-185X.1966.tb01501.x

Naven, R. T., Swiss, R., Klug-Mcleod, J., Will, Y., and Greene, N. (2013). The development of structure-activity relationships for mitochondrial dysfunction: uncoupling of oxidative phosphorylation. *Toxicol. Sci.* 131, 271–278. doi:10.1093/toxsci/kfs279

Neumcke, B., and Bamberg, E. (1975). "The action of uncouplers on lipid bilayer membranes," in *Lipid bilayers and biological membranes: dynamic properties* (New York: Dekker), 215–253.

Nielson, D. W., Goerke, J., and Clements, J. A. (1981). Alveolar subphase pH in the lungs of anesthetized rabbits. *Proc. Natl. Acad. Sci.* 78, 7119–7123. doi:10.1073/pnas.78.11.7119

Njire, M., Wang, N., Wang, B., Tan, Y., Cai, X., Liu, Y., et al. (2017). Pyrazinoic acid inhibits a bifunctional enzyme in *Mycobacterium tuberculosis*. *Antimicrob. Agents Chemother.* 61, 000700–17. doi:10.1128/AAC.00070-17

Norman, C., Howell, K. A., Millar, A. H., Whelan, J. M., and Day, D. A. (2004). Salicylic acid is an uncoupler and inhibitor of mitochondrial electron transport. *Plant Physiol.* 134, 492–501. doi:10.1104/pp.103.031039

Nyberg, K., Johansson, U., Johansson, A., and Camner, P. (1992). Phagolysosomal pH in alveolar macrophages. *Environ. Health Perspect.* 97, 149–152. doi:10.1289/ehp.9297149

Peters, B. J., Groninger, A. S., Fontes, F. L., Crick, D. C., and Crans, D. C. (2016). Differences in interactions of benzoic acid and benzoate with interfaces. *Langmuir* 32, 9451–9459. doi:10.1021/acs.langmuir.6b02073

Peterson, N. D., Rosen, B. C., Dillon, N. A., and Baughn, A. D. (2015). Uncoupling environmental pH and intrabacterial acidification from pyrazinamide susceptibility in *Mycobacterium tuberculosis*. *Antimicrob. Agents Chemother.* 59, 7320–7326. doi:10.1128/AAC.00967-15

Preiss, L., Langer, J. D., Yildiz, Ö., Eckhardt-Strelau, L., Guillemont, J. E. G., Koul, A., et al. (2015). Structure of the mycobacterial ATP synthase F_o rotor ring in complex with the anti-TB drug bedaquiline. *Sci. Adv.* 1, e1500106. doi:10.1126/sciadv.1500106

Salfinger, M., and Heifets, L. B. (1988). Determination of pyrazinamide MICs for *Mycobacterium tuberculosis* at different pHs by the radiometric method. *Antimicrob. Agents Chemother.* 32, 1002–1004. doi:10.1128/AAC.32.7.1002

Santucci, P., Aylan, B., Botella, L., Bernard, E. M., Bussi, C., Pellegrino, E., et al. (2022). Visualizing pyrazinamide action by live single-cell imaging of phagosome acidification and *Mycobacterium tuberculosis* pH homeostasis. *mBio* 13, e0011722. doi:10.1128/mbio.00117-22

Schaller, A., Sun, Z., Yang, Y., Somoskovi, A., and Zhang, Y. (2002). Salicylate reduces susceptibility of *Mycobacterium tuberculosis* to multiple antituberculosis drugs. *Antimicrob. Agents Chemother.* 46, 2636–2639. doi:10.1128/AAC.46.8.2636-2639.2002

Schoeman, J. F., Janse van Rensburg, A., Laubscher, J. A., and Springer, P. (2011). The role of aspirin in childhood tuberculous meningitis. *J. Child. Neurol.* 26, 956–962. doi:10.1177/0883073811398132

Scorpio, A., and Zhang, Y. (1996). Mutations in *pncA*, a gene encoding pyrazinamidase/nicotinamidase, cause resistance to the antituberculous drug pyrazinamide in tubercle bacillus. *Nat. Med.* 2, 662–667. doi:10.1038/nm0696-662

Shi, W., Chen, J., Feng, J., Cui, P., Zhang, S., Weng, X., et al. (2014). Aspartate decarboxylase (PanD) as a new target of pyrazinamide in *Mycobacterium tuberculosis*. *Emerg. Microbes Infect.* 3, e58–8. doi:10.1038/emi.2014.61

Shi, W., Zhang, X., Jiang, X., Yuan, H., Lee, J. S., Barry, C. E., et al. (2011). Pyrazinamide inhibits trans-translation in *Mycobacterium tuberculosis*. *Science* 333, 1630–1632. doi:10.1126/science.1208813

Shoeb, H. A., Bowman, B. U., Ottolenghi, A. C., and Merola, A. J. (1985). Enzymatic and nonenzymatic superoxide-generating reactions of isoniazid. *Antimicrob. Agents Chemother.* 27, 408–412. doi:10.1128/AAC.27.3.408

Sipe, H. J., Jaszewski, A. R., and Mason, R. P. (2004). Fast-flow EPR spectroscopic observation of the isoniazid, iproniazid, and phenylhydrazine hydrazyl radicals. *Chem. Res. Toxicol.* 17, 226–233. doi:10.1021/tx0341759

Tabata, K. (1962). Toxicity of ammonia to aquatic animals with reference to the effect of pH and carbonic acid. *Bull. Tokai Reg. Fish. Res. Lab.* 34, 67–74.

Takayama, K., Wang, L., and David, H. L. (1972). Effect of isoniazid on the *in vivo* mycolic acid synthesis, cell growth, and viability of *Mycobacterium tuberculosis*. *Antimicrob. Agents Chemother.* 2, 29–35. doi:10.1128/AAC.2.1.29

Timmins, G. S., Master, S., Rusnak, F., and Deretic, V. (2004). Requirements for nitric oxide generation from isoniazid activation *in vitro* and inhibition of mycobacterial respiration *in vivo*. *J. Bacteriol.* 186, 5427–5431. doi:10.1128/JB.186.16.5427-5431.2004

Vilaplana, C., Marzo, E., Tapia, G., Diaz, J., Garcia, V., and Cardona, P.-J. (2013). Ibuprofen therapy resulted in significantly decreased tissue bacillary loads and increased survival in a new murine experimental model of active tuberculosis. *J. Infect. Dis.* 208, 199–202. doi:10.1093/infdis/jit152

Wade, M. M., and Zhang, Y. (2006). Effects of weak acids, UV and proton motive force inhibitors on pyrazinamide activity against *Mycobacterium tuberculosis in vitro*. *J. Antimicrob. Chemother.* 58, 936–941. doi:10.1093/jac/dkl358

Wengenack, N. L., and Rusnak, F. (2001). Evidence for isoniazid-dependent free radical generation catalyzed by *Mycobacterium tuberculosis* KatG and the isoniazid-resistant mutant KatG(S315T). *Biochemistry* 40, 8990–8996. doi:10.1021/bi002614m

Winder, F. G. A., Collins, P., and Rooney, S. A. (1970). Effects of isoniazid on mycolic acid synthesis in *Mycobacterium tuberculosis* and on its cell envelope. *Biochem. J.* 117, 27P. doi:10.1042/bj1170027Pa

World Health Organization (2018). *Global tuberculosis report 2018*. Geneva: WHO.

Yano, T., Kassovska-Bratinova, S., Teh, J.-S., Winkler, J., Sullivan, K., Isaacs, A., et al. (2010). Reduction of clofazimine by mycobacterial type 2 NADH:Quinone oxidoreductase: a pathway for the generation of bactericidal levels of reactive oxygen species. *J. Biol. Chem.* 286, 10276–10287. doi:10.1074/jbc.M110.200501

Zhang, Y., and Mitchison, D. (2003). The curious characteristics of pyrazinamide: a review. *Int. J. Tuberc. Lung Dis. Off. J. Int. Union Tuberc. Lung Dis.* 7, 6–21.

Zhang, Y., Permar, S., and Sun, Z. (2002). Conditions that may affect the results of susceptibility testing of *Mycobacterium tuberculosis* to pyrazinamide. *J. Med. Microbiol.* 51, 42–49. doi:10.1099/0022-1317-51-1-42

Zhang, Y., Zhang, H., and Sun, Z. (2003). Susceptibility of *Mycobacterium tuberculosis* to weak acids. *J. Antimicrob. Chemother.* 52, 56–60. doi:10.1093/jac/dkg287

Zheng, J., Rubin, E. J., Bifani, P., Mathys, V., Lim, V., Au, M., et al. (2013). *para*-aminosalicylic acid is a prodrug targeting dihydrofolate reductase in *Mycobacterium tuberculosis*. *J. Biol. Chem.* 288, 23447–23456. doi:10.1074/jbc.M113.475798